

Kim Tien Nguyen

Mem. ASME

School of Mechanical Engineering,
Chonnam National University,
Gwangju 500-757, Korea
e-mail: nguyentien90@gmail.com**Seong Young Ko**

Mem. ASME

School of Mechanical Engineering,
Chonnam National University,
Gwangju 500-757, Korea
e-mail: sko@jnu.ac.kr**Jong-Oh Park**

Mem. ASME

School of Mechanical Engineering,
Chonnam National University,
Gwangju 500-757, Korea
e-mail: jop@jnu.ac.kr**Sukho Park¹**

Mem. ASME

School of Mechanical Engineering,
Chonnam National University,
Gwangju 500-757, Korea
e-mail: spark@jnu.ac.kr

Miniaturized Terrestrial Walking Robot Using PVDF/PVP/PSSA Based Ionic Polymer–Metal Composite Actuator

This paper presents a design and fabrication of millimeter scale walking robot using ionic polymer–metal composite (IPMC) actuator as the robot's leg for walking in terrestrial environment. A small scale of new IPMC actuator based on poly-vinylidene fluoride (PVDF)/polyvinyl pyrrolidone (PVP)/polystyrene sulfonic acid (PSSA) blend membrane was fabricated and employed in this study to sustain and drive the walking robot with sufficient force and displacement. The PVDF/PVP/PSSA based IPMC actuator with a polymer mixture ratio of 15/30/55 shows improved performances than Nafion based IPMC actuator. To enhance a traction force of the walking robot and to increase the life time of IPMC actuators, the IPMC strips are covered with a thin PDMS (polydimethylsiloxane) layer. A miniaturized terrestrial walking robot (size: 18 × 11 × 12 mm, weight: 1.3 g) with a light weight robot's body which can support 2-, 4-, or 6-IPMC-leg models was designed and implemented the walking motion on the ground at the maximum speed of 0.58 mm/s. [DOI: 10.1115/1.4032407]

Keywords: ionic polymer–metal composite actuator, PVDF, PVP, PSSA, terrestrial walking robot

1 Introduction

IPMC actuator is a type of wet ionic electro-active polymers (EAPs) that is typically composed of a thin ion-exchange membrane between two noble metal electrodes (e.g., platinum, gold, silver, etc.) [1]. Generally, IPMC actuator can be used in many bio-inspired aquatic systems or biomedical applications because of its superior properties, such as low actuation voltage, large tip displacement, light weight, well working in aquatic environment, ease of miniaturization, actuation and sensing capabilities, etc. Under electrical field, the mobile cations gathering with water molecules were redistributed from one electrode surface to the other one, resulting in the imbalance internal stresses inside the backbone membrane. At the cation-poor-region, polymer chains are contracted, while at the cation-rich-region, they are extended, causing the IPMC to bend to the anode side. On the other hand, when applying mechanical force to the IPMC, the moving of the mobile cations cause an electrical charge at each electrode. This can explain both the actuation and sensing characteristics of IPMCs [2].

However, the tip force generated by an IPMC is very small, and the loss of water molecules while working in air is a limitation of this potential actuator. Therefore, most of the bio-inspired systems using IPMCs as the actuators or sensors are operated in aquatic environments where the actuating force is no longer problematic with the aid of buoyancy, and the system works well without any loss of water molecules inside. Several swimming bio-inspired robots were reported as follows: First, fish-like robots that can swim in the water by using an IPMC as the fish tail have been developed [3–5], and a ray-like swimming robot mimicked the pectoral fin of a ray using IPMC strips has been reported [6,7]. Second, Najem et al. [8] and Gou et al. [9] designed the jellyfish type of swimming robot using IPMCs to mimic the jellyfish motion. Finally, Kamamichi et al. [10] reported a snake-like

swimming robot that consists of two IPMC strips and applied periodically input with an appropriate frequency and phase shift to realize the snake-like swimming motion.

Contrary to swimming motion, walking motion aimed at moving across many kinds of terrains, not only in aquatic environments but also in terrestrial environments. However, the main concern for a terrestrial walking robot is how to support and move the robot body, especially a bio-inspired walking robot using IPMCs. Many researchers concentrated their efforts on the design of a robot structure and walking mechanism in order to apply this potential IPMC to the bio-micro walking robot. Chang et al. used thick Nafion based IPMCs (1 mm) to generate sufficient force for a walking robot. The walking robot (size: 102 × 80 × 43 mm, weight: 39 g) with 6 two-degrees-of-freedom (2DOF) legs was designed, implemented, and walked in water at the speed of 0.5 mm/s [11]. Another report [12] introduced an underwater microrobot with multifunctional locomotion that used ten IPMC actuators to realize walking, rotating, and grasping motions. In aquatic environment, with the aids of buoyancy, these walking robots do not need to deal with the bucking force and blocking force problem in order to support those heavy weight robot's bodies and drive the robot motion. Moreover, the ground contact is not the primary concern for walking robot in aquatic environment because of the surrounding water. However, in terrestrial environment, especially at a millimeter scale, where the friction force governs all the motions, the ground contact plays an important role in locomotion of the robot. Thus, the slipping is one of the biggest problems of terrestrial walking robot.

Many different terrestrial walking robots using the other smart materials are developed. One of the most popular smart materials, shape memory alloy (SMA) actuator has been used to build the walking robot because of its lightweight, large actuating force, and good mechanical properties [13–15]. With fast response, high locomotive power properties, piezoelectric ceramics actuators are widely applied in walking robot, such as HARM² [16], HARM³ [17], and HARM-VP [18]. However, there are some disadvantages that limit these smart materials in biomedical applications, such as the heat generating by SMA in heating process, the high

¹Corresponding author.

Manuscript received August 12, 2015; final manuscript received December 21, 2015; published online March 7, 2016. Assoc. Editor: Robert J. Wood.

actuation voltage of piezoelectric actuator which can damage the human tissues. The ionic EAPs can work overall in robot mission time without degradation, corrosion, or wear in the chemical environment (enzyme, pH, and under lymphocyte action), thus is suitable for medical application which require inert materials, such as platinum, Nitinol (NiTi), some stainless steels, ceramic alumina, and some polymers. Of course, this material should be nontoxic with no damage to the human body at a low actuation voltage [19].

The goal of this work is to address these engineering challenges in order to develop a low-power terrestrial walking robot capable of flat ground locomotion, and suitable for medical application. The proposed IPMC actuator based on PVDF/PVP/PSSA with polymeric mixture ratio of 30/15/55 was fabricated and its performance was characterized. For a walking robot, we chose the best size, thickness of IPMC actuator to ensure the sufficient force and displacement. In addition, the detailed design and fabrication of the proposed walking robot structure, the walking mechanism and control system will be explained in this paper through five sections. In detail, the fabrication process and property analyses of our IPMC based on PVDF/PVP/PSSA will be presented in Sec. 2. Section 3 describes the bio-inspired walking robot structure design, control system and its walking mechanism. The experimental results of the walking robot on the flat surface at various input frequency were shown in Sec. 4. Finally, Sec. 5 focused on conclusions.

2 PVDF/PVP/PSSA Based IPMC Actuator for Terrestrial Walking Robot

2.1 Fabrication and Property Analysis of IPMC actuator.

There are many factors that affect the IPMC actuator and cause its nonlinear behavior, such as membrane conditions, surface conditions, conductivity, size, and driving voltage. The ion exchange membrane condition plays a vital role to IPMC performance, which decides how much mobile cations and absorbed water molecules are included in the membrane of IPMC. By controlling the membrane condition, the characteristics and performance of IPMC can be generally determined. The proposed blend membrane based on PVDF/PVP/PSSA with a ratio of 30/15/55 has shown better performance in comparison with a conventional Nafion-based membrane [20].

To prepare the blend membrane, the polymeric components such as PVDF, PVP in powder form and PSSA liquid form were dissolved with *N,N* dimethyl formamide (Sigma Aldrich) to form a 10 wt. % membrane mixture solution. The blend membrane was fabricated by a casting method and two electrodes on the both sides of the blend membrane were created, where the electroless plating method was selected because of the nonconductivity properties of the proposed membrane. The following ingredients must be prepared, such as Tetra-amine platinum(II) chloride hydrate ($[\text{Pt}(\text{NH}_3)_4]\text{Cl}_2 \times \text{H}_2\text{O}$) (Sigma Aldrich), sodium borohydride (NaBH_4), lithium chloride (LiCl), hydroxylammonium chloride ($\text{HONH}_2 \cdot \text{HCl}$), hydrochloric acid (HCl), and ammonium hydroxide (NH_4OH) (DAE-JUNG, Korea). IPMC fabrication procedures were adopted from the previous works [20–23] and were enhanced to ensure sufficient force and displacement for robotics applications. Especially, the platinum electrode coating process (second reduction) was repeated twice, which causes the uniform surface layer thickness, the low resistance, and the high conductivity of the electrodes. Our fabrication method provided 10–20 μm uniform platinum layers and the surface resistance around 0.2 Ω/mm . Therefore, it was expected that the proposed IPMC actuator has the enhanced displacement and the increased blocking force.

In order to measure IPMC responses, a data acquisition system was prepared and set up, as shown in Fig. 1. As a data acquisition system, a digital signal-processing board (DS1103, dSPACE) linked to a computer was introduced. For the deflection

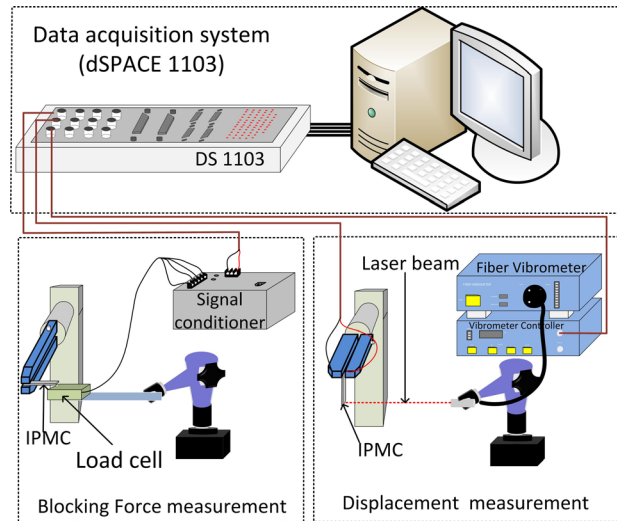


Fig. 1 Experimental setup for IPMC bending test and blocking force test

measurement of IPMC actuator, DS1103 board was connected to a laser vibrometer (Model No.-OFV-2510, Polytec) and to the electrodes of the IPMC's clamping devices. A load cell (GSO-10, Transducer Techniques) with capacity of 10 g and load cell signal conditioner (TMO-2, Transducer Techniques) were used to measure the blocking force of IPMC actuator. The measured data were acquired using real-time interface CONTROLDESK software (dSPACE) and linked to MATLAB for analysis throughout the experiment.

In this work, many experiments had been implemented to control the deflection of the IPMC actuator by changing its size. IPMC actuators with widths 2–4 mm, and the following 10, 15, and 20 mm in lengths, are fabricated. In Figs. 2(a) and 2(b), when increasing the width of IPMC actuator from 2 mm up to 4 mm, the displacement of IPMC actuator is decreased from 3.8 mm down to 2.8 mm (with 20 mm sample's length), from 3.1 mm to 2 mm (with 15 mm sample's length), and 2.1 mm to 1.12 mm (with 10 mm sample's length), whereas the blocking force are increased from 7.22 mN up to 13 mN with samples of 20 mm in length, from 9.1 mN up to 15.2 mN with samples of 15 mm in length, and from 10.3 mN up to 18.2 mN with samples of 10 mm in length. In contrast with increasing the width, when increasing the length of IPMC actuators, it is obviously demonstrated that the displacement is strongly increased whereas the blocking force is decreased (Fig. 2(b)). Based on the response of IPMC actuator, the size 15 mm in length and 4 mm in width is chosen to ensure the proficient displacement and blocking force for walking robot. The sample's thickness used in these experiments is 0.35 mm. Figure 2(c) demonstrates the relation of IPMC thickness to displacement and blocking force. The IPMC samples with different thicknesses (0.2, 0.25, 0.3, 0.35, 0.4, 0.5, 0.6, 0.7, 0.8, 0.9, and 1 mm) are fabricated, tested to choose the proficient thickness IPMC leg for terrestrial walking robot. In Fig. 2(c), the blocking force is increased from 10 mN up to 32 mN, and the displacement is decreased from 4.1 mm down to 0.42 mm, when the thickness is increased from 0.2 mm to 1 mm. The sample's thickness of 0.35 mm is the most suitable thickness for IPMC leg, which ensures the sufficient blocking force and displacement as well as the flexibility for IPMC legs. Finally, the 15 mm \times 4 mm \times 0.35 mm IPMC legs are chosen for the walking robot.

The IPMC actuator was tested using square-wave input signal with amplitude of 3 V, actuation frequency of 0.05 Hz which aims to test the displacement and blocking force under low actuation voltage (Fig. 3(a)). In part (i), the IPMC shows the bending response with about 2 mm tip displacement. The data in part (ii) shows the blocking force response of IPMC actuator.

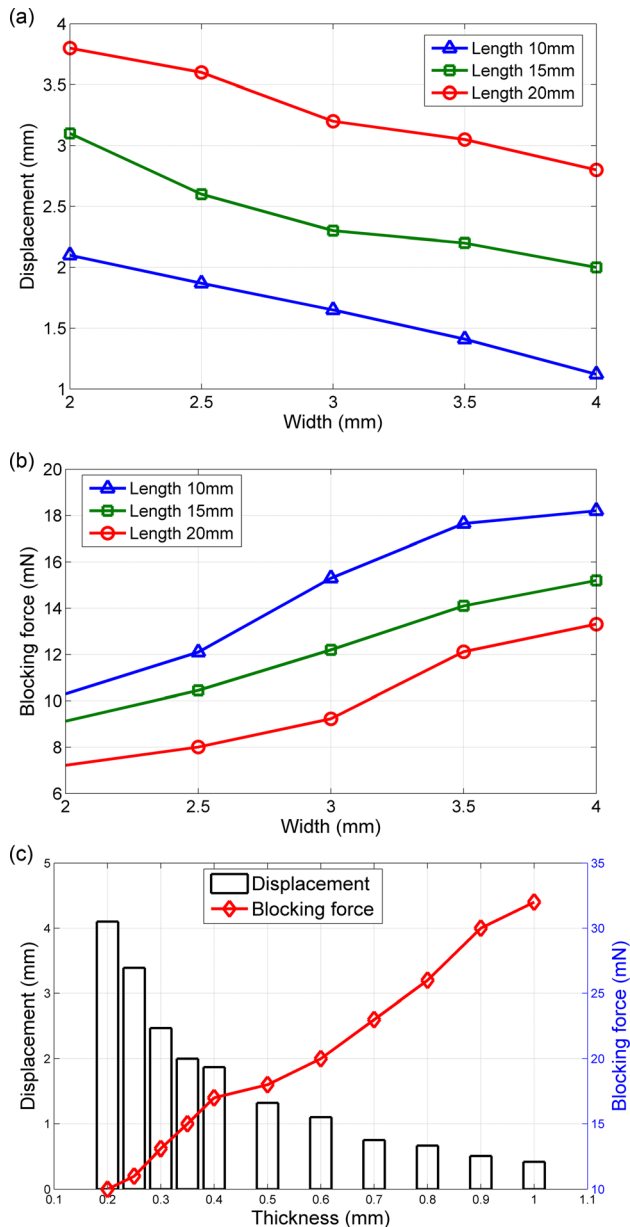


Fig. 2 (a) Displacement response, (b) blocking force response of IPMC actuator with different width and length, and (c) displacement and blocking force response of IPMC actuator with different thickness

The maximum blocking force is demonstrated on the figure as about 15 mN force.

The IPMC actuator was carefully characterized the performance with the desired actuation voltage 5 V DC and AC signal. Figure 3(b) shows the experimental results of IPMC actuators under a 5 V square-wave input and various actuation frequencies from 0.1 to 1 Hz. This experiment aims to characterize the force and displacement responses of IPMC actuator under various actuation frequencies for walking robot. It shows that the displacement and blocking force of the IPMC actuator are inversely proportional to the actuation frequency, i.e., when we increase the actuation frequency, the displacement and the blocking force of the IPMC actuator are decreased. At 0.1 Hz, our proposed IPMC actuator shows 4 mm in displacement and 16 mN in blocking force, whereas the displacement and blocking force are decreased to 0.5 mm and 5 mN at 1 Hz, respectively. The square-wave input signal was chosen in this experiment because it creates the

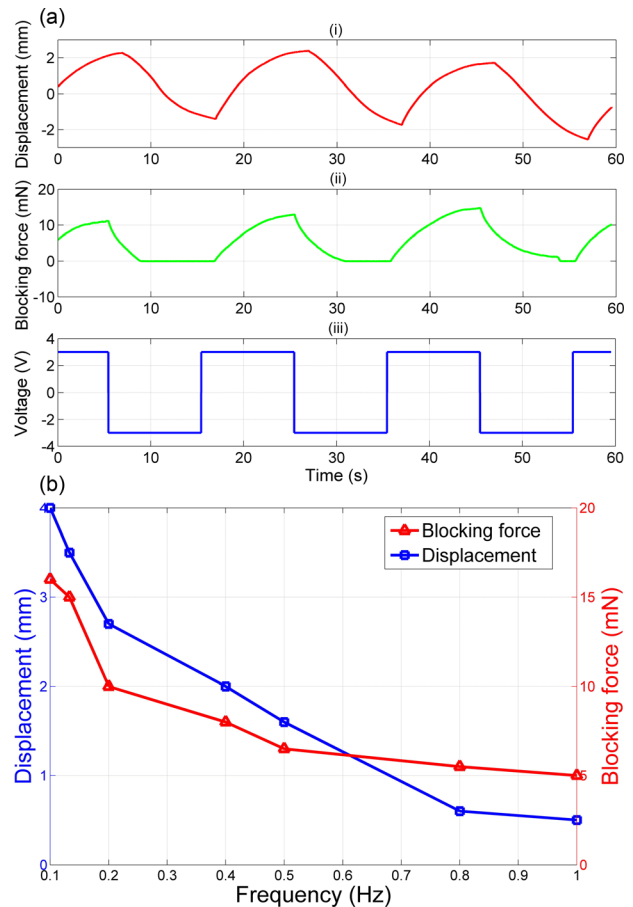


Fig. 3 (a) Displacement and blocking force response of IPMC actuator under 3V, 0.05Hz input signal and (b) response of IPMC under various input signals (5V, 0.1–1 Hz)

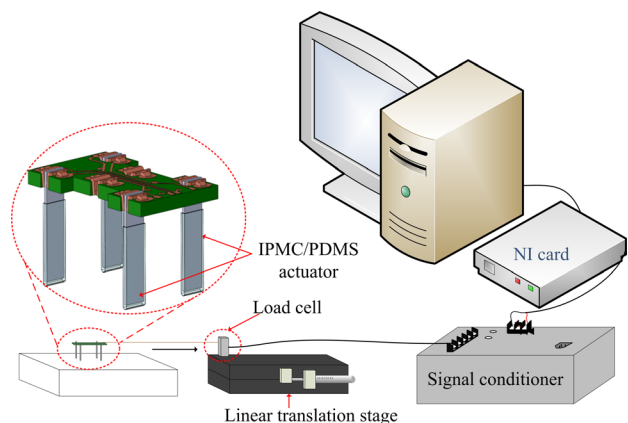


Fig. 4 Experimental setup for friction force test between walking robot and ground

greatest force and displacement, as well as the fastest response, in comparison with sinusoidal and saw-tooth wave input signals.

2.2 Enhance IPMC Actuator Performance Using PDMS Coating Method. In micro- and mesoscales, the surface friction force plays a very important role in the interactions between objects. Especially in a walking robot, the friction between the robot's legs and the ground decides the efficiency of the robot motion. Developing of the walking robot without careful considering the friction between robot's leg and the ground will lead to the

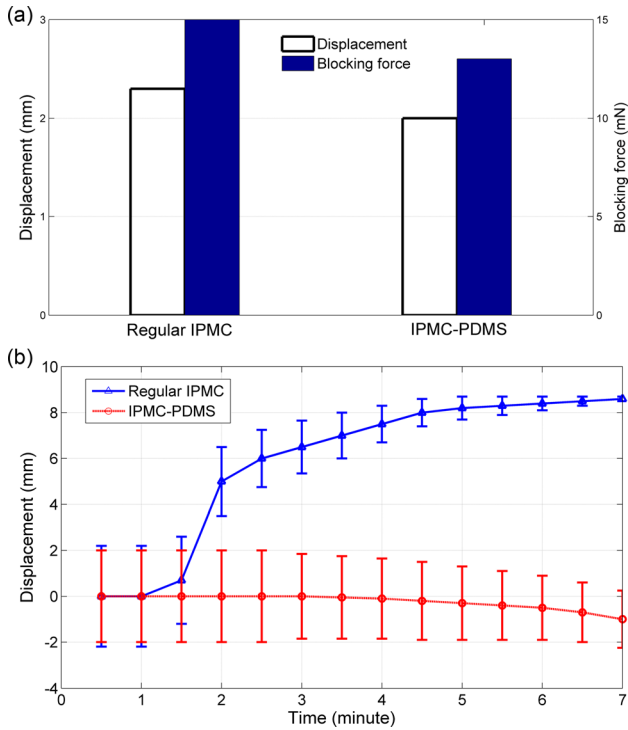


Fig. 5 (a) Displacement and blocking force response of regular and IPMC-PDMS actuator and (b) life-time cycle of regular IPMC actuator and IPMC-PDMS actuator

slipping problem, which cause the slowed locomotion. The loss of ground contact between the IPMC leg and the ground was the main reason for this problem.

In order to solve this slipping problem, we adopted a thin PDMS polymer layer to cover the IPMC leg, which can easily bend and come in full contact with the walking plane, no matter how great the contact angle. PDMS is appropriate for use in this situation because of its flexible properties and easy fabrication process. The dipping method is used to coat the PDMS layer outside of the IPMC actuator. First, a PDMS solution with a ratio of 10:1 Sylgard 184 A, i.e., a silicone elastomer base, and Sylgard 184B, i.e., a silicone elastomer curing agent, was prepared. Then, the IPMC actuators were immersed into the PDMS solution to cover about 80% of the length of the IPMC, leaving 20% for attaching the electrodes. The IPMCs with the PDMS coating (called IPMC-PDMS) were hung in the oven at 80 °C for 1 h. Then, the IPMC actuators with a thin PDMS layer are reserved in the deionized (DI) water for the actuation test.

Four IPMC actuators with PDMS coating (IPMC-PDMS) were assembled in the walking robot, and the load cell (GSO-10, Transducer Techniques) was connected to the walking robot using a thin wire for the measurement of the friction and propulsion force, as shown in Fig. 4. The linear translational stage was adjusted to increase the tension on the wire that connects the load cell and the walking robot, until the walking robot starts to slide. At that moment, the maximum friction force between the robot leg and the ground can be measured and recorded. We repeated this experiment many times with IPMC-PDMS and IPMC actuators to compare their performances. The experimental results demonstrated that the walking robot using IPMC-PDMS showed greater friction force than that using IPMC alone. That is, the friction

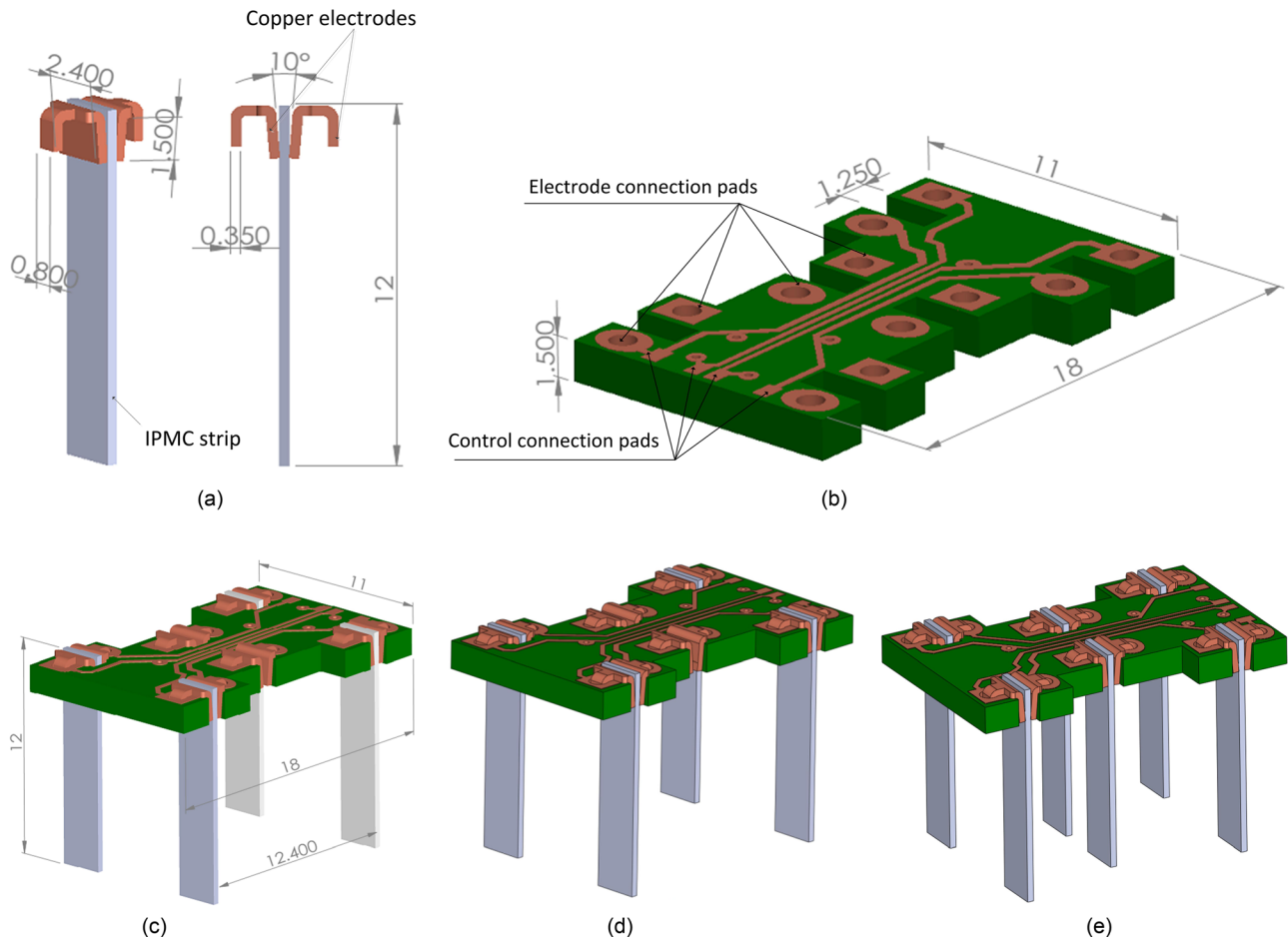


Fig. 6 (a) Structure of IPMC leg connectors, (b) PCB-robot body; design of IPMC walking robot, (c) 2-IPMC-leg model, (d) 4-IPMC-leg model, and (e) 6-IPMC-leg model

coefficient of IPMC-PDMS on the Teflon surface is about 0.456 on average, which is larger than twice the value of IPMC alone (0.21). They showed that an IPMC-PDMS actuator has better ground contact than IPMC, and therefore, the slipping of the IPMC walking robot is reduced. Moreover, by coating a thin PDMS layer outside of the IPMC actuator, the ground contact was improved, the motion was not disturbed. We compared a regular IPMC actuator and the IPMC-PDMS actuator through the displacement tests, blocking force tests, and life-time cycle tests. As a result of thin PDMS coating, the IPMC-PDMS actuator shows a slightly unfavorable response in comparison with the regular IPMC actuator (Fig. 5(a)). That is, the regular IPMC actuator showed 2.3 mm tip displacement and 15 mN blocking force, but the IPMC-PDMS actuator showed 2 mm tip displacement and 13 mN blocking force. However, the life-time cycle of IPMC-PDMS actuator was clearly enhanced. As shown in Fig. 5(b), when we test the two actuators with the actuation frequency of 0.4 Hz, the IPMC-PDMS actuator bended steadily after 3.5 min, then gradually declined its performance and showed a lightly drift from the initial stage after 7 min, whilst the regular IPMC actuator showed the steady bending motion in 80 s, then dramatically changed its shape, significant drift from initial stage at 2 min, and strongly decreased its performance, became brittle after 7 min due to the leakage of water out of the membrane in actuation process.

3 Design and Fabrication of Miniaturized Terrestrial Walking Robot Using IPMC

3.1 Walking Robot Structure. In robot's mechanical design, many lightweight and simple robot's structures have been considered, such as wood, plastic, or composite based robot's structure. Especially in milliscale robot, where a large number of control circuit and complex connection need to be populated in a small area, the robot's structure plays an important role in robot motion. In order to solve this problem, a printed circuit board (PCB) was designed and used as the robot's body, upon which all the mechanic parts, electrode connection pads, and control connection pads and actuators were installed [13–18,24]. A 1.5 mm thick double-sided circuit board is used for this purpose, resulting in a weight of about 520 mg unpopulated board (Fig. 6(b)).

In experiments of IPMC actuator, clamping pressure between the IPMC and the clamping device will strongly affect the actuation performance of the IPMC actuators because electrical contact resistance between two electrodes of the IPMC and the clamping device and material properties will be greatly changed according to the change of clamping pressures [25]. Therefore, in biosystem using IPMC and IPMC robot, the design of the electrodes that connected between IPMC and system is very important. It not only sustains the clamping pressure on IPMC, but ensures the uniform contact between electrodes and IPMC as well. Figure 6(a) illustrates the structure of IPMC leg connectors which were cut from the copper plate (0.35 mm thickness). A pair of copper connectors is bent with contact angle 10 deg and fixed to the robot's body by manual soldering with the distance 0.3 mm from each other in order to provide enough clamping pressure on IPMC, easy to assembly, disassembly as well as no damage to the IPMC surface.

The final design of walking robot are showed in Fig. 6 with dimension of 18 mm length \times 11 mm width \times 12 mm height. On the robot's body, six pair of copper connectors were symmetrically designed and placed, in order to fix 2-, 4-, or 6-IPMC legs to the robot's body, resulting in the 2-, 4-, or 6-IPMC-leg models (Figs. 6(c)–6(e)). In 2-IPMC-leg model, two IPMC legs are inserted into two front connectors to generate the motion for robot, and two dummy legs, made of acrylonitrile butadiene styrene (ABS) plastic, are fixed to two rear connectors to keep balance for robot during the walking motion. The IPMC legs using in this application with dimensions of 15 mm \times 4 mm \times 0.35 mm were selected in Sec. 2. This proposed structure can easily

switched from 2-IPMC-leg model to 4-, or 6-IPMC-leg models by assembly two or four more IPMC legs. In this work, 2-, 4-, or 6-IPMC-leg models are applied to characterize the locomotion of the walking robot.

3.2 Electronics for IPMC Actuation. In this work, for the controlling of the walking robot, an external control circuit, which consists of locomotion generator, drive stage, and programming interface, was designed to generate the control signal and sustain the power for IPMC actuators. The proposed IPMC leg for walking robot has absorbed current around 100 mA when it operates. The instant maximum current, around 200 mA, occurs when the voltage abruptly changes in square wave control signal. Therefore, with 6-IPMC-leg model, the maximum absorbed current can rise up to 1.2 A, when six IPMC legs are simultaneously activated. However, the other IPMC strips using Nafion-based IPMC actuator [11] required much higher operating current at around 500 mA and instant maximum current at nearly 1.5 A.

In order to supply that high current control signal to the actuators, a drive stage was designed using an edited H-bridge circuit

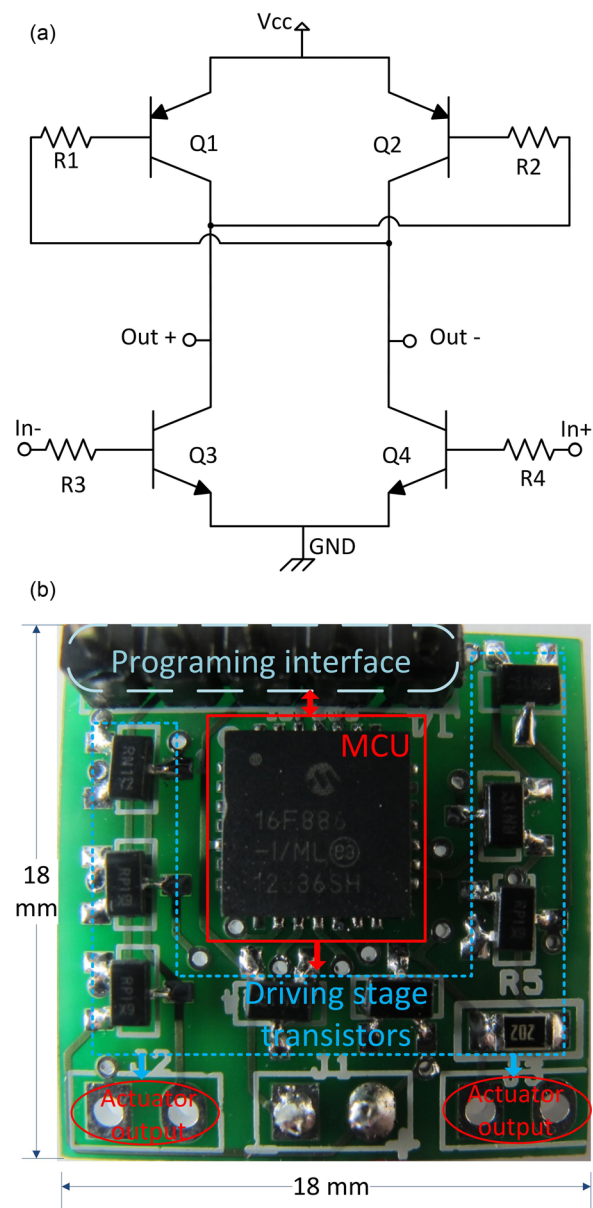


Fig. 7 (a) Detailed schematic of the drive stage for IPMC actuators and (b) populated control circuit for walking robot

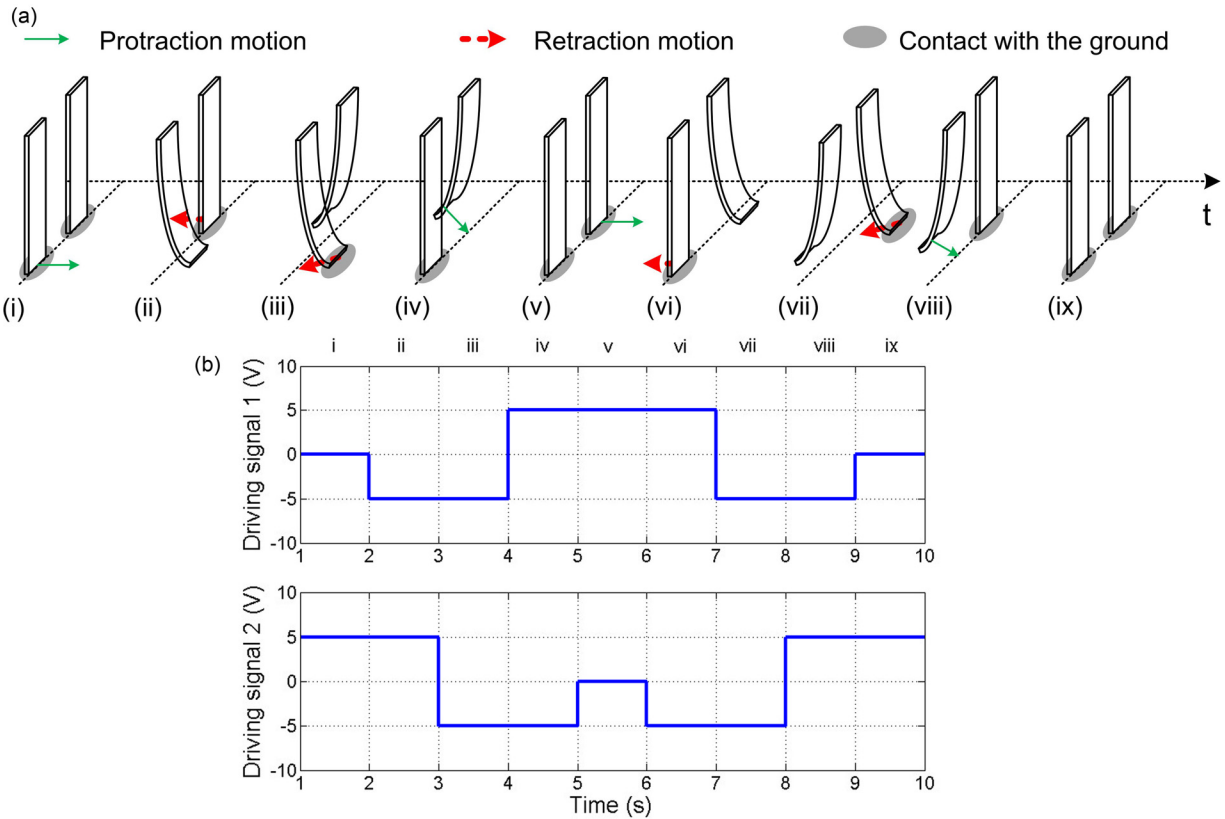


Fig. 8 (a) Locomotion of walking robot; (b) sequence control signal for the walking robot

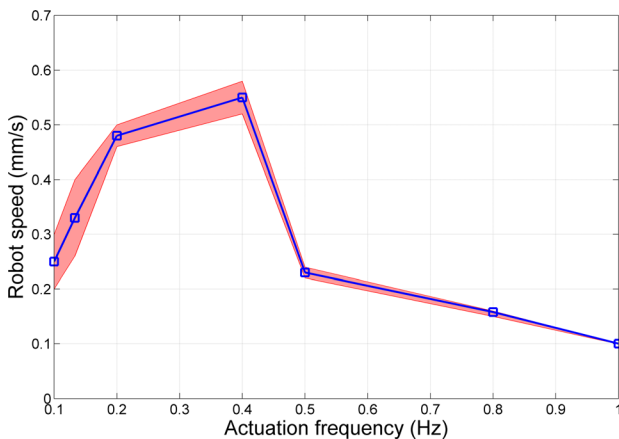


Fig. 9 The speed trial results were obtained for 0.1–1 Hz actuation frequencies. The data points show the steady results, whereas the error area shows the maximum and minimum trial speed values.

with bipolar junction transistors PNP 2DB1694 (Q1, Q2) and NPN 2DD2656 (Q3, Q4), manufactured by Diodes Incorporated. In Fig. 7(a), the drive transistor resistors are designed as $R1 = R2 = R3 = R4 = 2 \text{ k}\Omega$, in order to provide the maximum supply current of around 2 A, that ensure the power for IPMC actuators. The drive stage amplifies the current of the sequence control signal from microcontroller (PIC16F886, 8 bit, manufactured by Microchip Technology, Inc.), but maintains the voltage gain as one. Two of these drive stage are used to drive 2, 4, or 6 IPMC actuators, which will be explained more detailed in Sec.

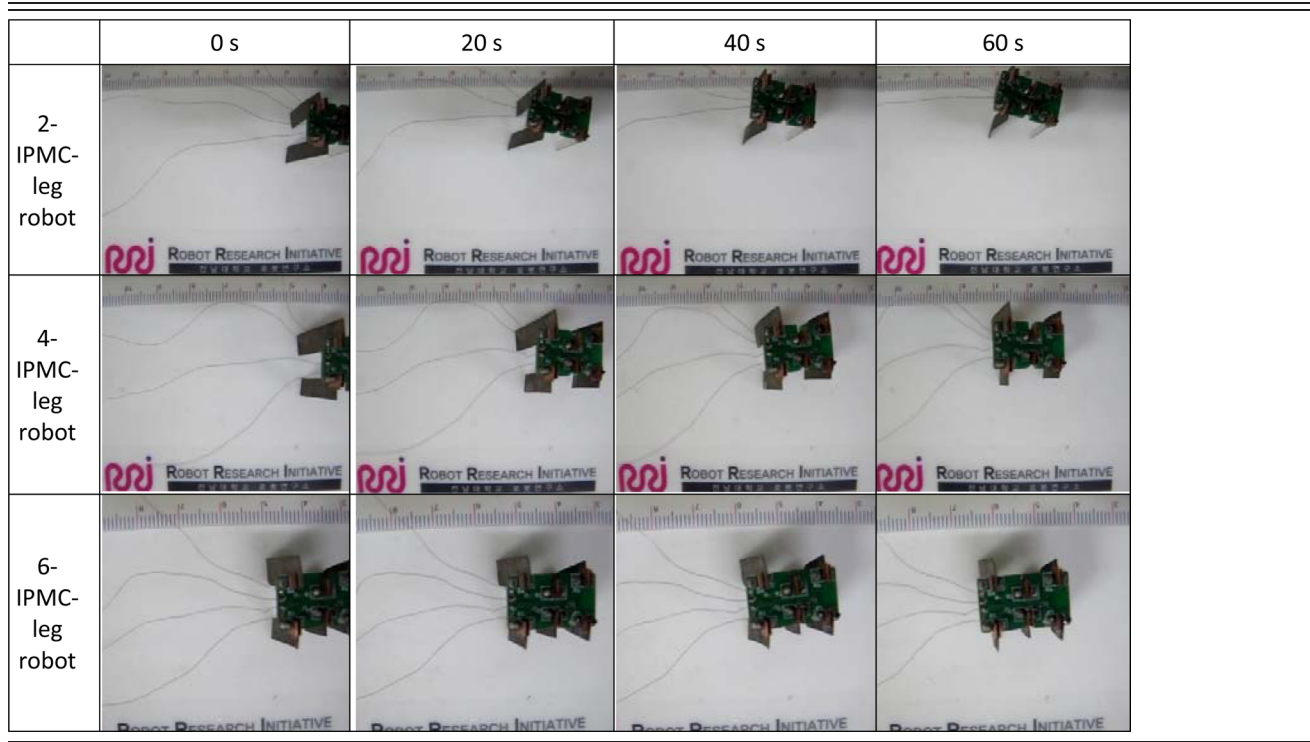
3.3. Finally, through the manual soldering, we created a populated circuit board with size of $18 \text{ mm} \times 18 \text{ mm}$ (Fig. 7(b)). This control circuit will be connected to the robot's body by four of 0.05 mm diameter copper wire (Nilaco, Japan) to transfer the control signals to each IPMC actuators.

3.3 Locomotion Sequence of Walking Robot. IPMC actuator can be considered as the continuum structure because of its bending motion. Thus, in this paper, we proposed a robot locomotion based on this bending motion to mimic the insect's walking motion. In order to design the locomotion sequence for 2-, 4-, and 6-IPMC-leg robots, the simplest locomotion, 2-IPMC-leg locomotion, is first considered as the background for further locomotion design of 4-, and 6-IPMC-leg models. The locomotion sequence of the robot using two IPMC actuators can be demonstrated by motion of two front legs as in Fig. 8(a). Part (i) is the initial state where both IPMC legs are touching the ground and then the right IPMC leg started to bend forward in order to prepare for the next step. In this step, the right IPMC leg is lift-off, the left IPMC leg and two rear dummy legs touch the ground that make a triangle between these three legs. The robot body was designed with the center of mass stay in this triangle to ensure the robot not collapse when it walking. In part (ii), the left IPMC leg which is touching the ground, bend backward (retraction motion) that exert a backward force to the ground, and therefore push the robot moving forward. The left IPMC keep bending backward, lower the robot body, and push the robot moving forward until the left and right legs touch the ground like part (iii), just then the right IPMC leg bend backward to the initial position, lift the body up, and once again push the robot moving forward. Part (iv) shows the forward bending motion of left leg back to the initial state. In order to keep robot move straight forward, part (v)–(ix) repeated the same procedure in part (i)–(iv), but in a symmetrical way, i.e., the left leg started to bend first. Fig 8(b) shows the driving signals for two

Table 1 Walking test

Prototype	Size (mm × mm × mm)	Weight (g)	Speed (mm/s) at driving frequency (Hz)						
			0.10	0.13	0.20	0.40	0.50	0.80	1.00
2-leg	18 × 11 × 12	1.26	0.25	0.35	0.48	0.58	0.25	0.18	0.10
4-leg	18 × 11 × 12	1.30		0.47					
6-leg	18 × 11 × 12	1.34		0.33					

Table 2 Frame capture of walking motion under sequence control signal 5 V, 0.13 Hz



IPMC legs to make the bending motion corresponding to the part (i)–(ix) in Fig. 8(a). These signals were generated by the control circuit which was showed in Sec. 3.2.

Based on the proposed locomotion for 2-IPMC-leg model, we designed the locomotion for 4-IPMC-leg robot by keeping two front IPMC legs, replacing two rear dummy legs by two other IPMC legs, and applying the same proposed locomotion sequence. In this prototype, two left legs are designed with the same locomotion sequence and driving signals, as well as two right legs. By inserting two other IPMC legs into the middle connectors of 4-IPMC-leg robot and applying the proposed locomotion sequence to six IPMC actuators, the tripod locomotion, 6-IPMC-leg robot locomotion can be created, where the left front leg, right middle leg, and left rear leg have the same locomotion sequence, driving signal, and vice versa. With 4-, and 6-IPMC-leg robot locomotion sequence, the walking robot can have theoretically increased locomotive power by double, or triple in comparison with 2-IPMC-leg model.

4 Experiments

A walking robot prototype has 1.3 g weight and 18 mm length × 11 mm width × 12 mm height and demonstrates walking motions on the flat ground. A number of ground surfaces were tested for walking such as paper, metal, plastic, and glass, where the walking robot showed the slipping or sticking and slowed or disturbed locomotion. Especially, Teflon surface was chosen

for walking performance test since it provided good results. The driving voltage is 5 V square-wave which can cause the larger deformation, force and faster response for IPMC actuator than the other signal because of abrupt change between peaks and troughs.

First of all, the regular IPMC legs were applied to walking robot to test its performance in terrestrial environment. However, the walking robot using regular IPMC legs showed slipping problem and losing of the ground contact between IPMC legs and the ground, which brought the walking robot to standstill in almost every experiments and reached the maximum speed, about 0.2 mm/s at 0.1 Hz in one trial. The walking robot using regular IPMC showed worse walking results when we increased the driving frequency.

Subsequently, the walking speed of the simplest model, 2-IPMC-leg robot with IPMC-PDMS legs, was characterized using our proposed locomotion sequence (described in Fig. 8(a)) at actuation frequencies from 0.1 to 1 Hz, the results of which are summarized in Fig. 9. The walking robot showed the walking speed at about 0.25 mm/s with driving frequency of 0.1 Hz. When increasing the actuation frequency, the walking speed also increased. And the optimal driving frequency of 0.4 Hz was found, where the walking robot walked on average of 0.55 mm/s and reached the maximum speed at around 0.58 mm/s in one trial. On the further frequencies, the walking robot showed fast decrease in speed due to the small blocking force and displacement of IPMC actuator at higher actuation frequency. As IPMC actuator performance highly depends on the actuation frequency

Table 3 Comparison of different types of walking robot

Robot	Type of actuator	Power (V)	Response times (Hz)	Speed
HAMR ³ [17]	Piezoelectric actuator	200	20	4.3 cm/s
ARRIpede [24]	Electrothermal actuator	25	65	3 mm/s
RoACH [15]	SMA	13.6	7.5	3 cm/s
MEMS microrobot [13]	SMA	3	2	0.325 mm/s
IPMC walking robot	IPMC	5	0.4	0.58 mm/s

in Fig. 3, the bigger the actuation frequency we apply to robot system, the smaller displacement and force can be generated in order for obtaining the efficient step at higher frequency (0.5–1 Hz). The walking robot motion at 0.5 Hz is the best evidence for this reason, at which the robot traveled straight for 15 mm at 0.25 mm/s before slowing down and standstill.

Then, the walking motion of 4- and 6-IPMC-leg robots are implemented under low actuation frequency, 0.13 Hz, to characterize their performance, and compare with 2-IPMC-leg model (Table 1). The 4-IPMC-leg model showed smooth walking motion in distance of 28 mm in 60 s, which is approximately 1.33 times faster than 2-IPMC-leg robot at the same actuation frequency (Table 2, second row). This result illustrates that the walking robot can increase the locomotive power and speed by using 4-IPMC-leg model.

However, the 6-IPMC-leg robot demonstrated a walking speed of 0.33 mm/s which is almost same to 2-IPMC-leg model (Table 2, third row). This 6-IPMC-leg model shows the opposite results to our expectation which supposes to be larger in locomotive power and speed. The walking performance of the walking robot is mainly limited by the performances of the IPMC actuators. And it is expected that the unidentified displacement is caused by the difference of the IPMC actuators such as its resistance, conductivity and shape. These differences in performance of IPMC actuator affected to walking results of 2-, 4-, and 6-leg design. Especially, when a larger number of IPMC legs, 6 legs in this work, were applied, it showed worse walking performance due to a larger number of different performance IPMC leg cause a larger restriction force or smaller pushing force than in 2- or 4-leg design. In addition, the PDMS coating of the proposed IPMC-PDMS can enhance the lifetime of IPMC actuator. The PVDF/PVP/PSSA based IPMC actuator with water as the solvent cannot operate for too long in air and need to be rehydrated [26]. This is also a limitation for 6-IPMC-leg robot, which requires more time to insert the IPMC legs into the robot.

The robot walking nearly moves straightforward in almost every case. However, the walking robot occasionally moves a little bit to the left or right. We expected that the different performances between left and right IPMC legs cause a crooked path of the walking robot. The effect of connection wires could be ignored because of its thin, lightweight properties and sufficient force generated by our fabricated IPMC based PVDF/PVP/PSSA blend membranes (Table 3).

5 Conclusions

A design and results of a walking robot with 2-, 4-, and 6-IPMC legs, which is capable of low-power terrestrial walking on the flat ground, have been presented. This study focuses on PVDF/PVP/PSSA-based IPMC actuator and design methodology of the walking robot based on various fundamental experiments such as bending tests, blocking force tests, and actuating tests on the effect of amplitude and actuation frequencies to IPMC response. Our PVDF/PVP/PSSA blend-membrane showed that the proposed IPMC can sustain and drive the walking robot body.

Despite the limitations mentioned in Sec. 4, the walking robot with lightweight and simple structure had proved the possibility to move on the flat ground using selected IPMC actuator, locomotion sequence, and driving signals. Therefore, the walking robot can be

a platform for further works forward the fully autonomous IPMC walking robot. The future work will address the limitations mentioned in Sec. 4, including the mechanic works and chemical works, in order to create an autonomous walking robot capable of walking in several terrains, forward to the biomedical application. For instance, the first improvement could be focused on improving IPMC's characteristics for longer lifetime in air by changing from the water based solvent to ionic liquid based solvent. Another future topic includes the integration of the microcontroller, sensor, power on the flexible circuit, and changing the mechanical design of the robot, which capable of controlling of the leg's motion curve.

Acknowledgment

This research was supported by NSL (National Space Lab) program through the National Research Foundation of Korea funded by the Ministry of Education, Science and Technology (2014034793).

References

- [1] Shahinpoor, M., Bar-Cohen, Y., Simpson, J. O., and Smith, J., 1998, "Ionic Polymer–Metal Composites (IPMCs) as Biomimetic Sensors, Actuators and Artificial Muscles—A Review," *Smart Mater. Struct.*, 7(6), pp. R15–R30.
- [2] Shahinpoor, M., and Kim, K. J., 2001, "Ionic Polymer–Metal Composites: I. Fundamentals," *Smart Mater. Struct.*, 10(4), pp. 819–833.
- [3] Aureli, M., Kopman, V., and Porfiri, M., 2010, "Free-Locomotion of Underwater Vehicles Actuated by Ionic Polymer Metal Composites," *IEEE-ASME Trans. Mechatronics*, 15(4), pp. 603–614.
- [4] Chen, Z., Shataru, S., and Tan, X., 2009, "Modeling of Biomimetic Robotic Fish Propelled by an Ionic Polymer–Metal Composite Caudal Fin," *IEEE-ASME Trans. Mechatronics*, 15(3), pp. 448–459.
- [5] Ye, X., Su, Y., Guo, S., and Wang, L., 2008, "Design and Realization of a Remote Control Centimeter-Scale Robotic Fish," *IEEE/ASME International Conference on Advanced Intelligent Mechatronics (AIM 2008)*, Xian, China, July 2–5, pp. 25–30.
- [6] Punning, A., Anton, M., Kruusmaa, M., and Aabloo, A., 2004, "A Biologically Inspired Ray-Like Underwater Robot With Electroactive Polymer Pectoral Fins," *International Conference on Mechatronics and Robotics*, Aachen, Germany, Sept. 13–15, pp. 241–245.
- [7] Chen, Z., Um, T. I., Zhu, J., and Bart-Smith, H., 2011, "Bio-Inspired Robotic Cownose Ray Propelled by Electroactive Polymer Pectoral Fin," *ASME Paper No. IMECE2011-64174*.
- [8] Najem, J., Sarles, S. A., Akle, B., and Leo, D. J., 2012, "Biomimetic Jellyfish-Inspired Underwater Vehicle Actuated by Ionic Polymer Metal Composite Actuators," *Smart Mater. Struct.*, 21(9), p. 094026.
- [9] Guo, S., Shi, L., Ye, X., and Li, L., 2007, "A New Jellyfish Type of Underwater Microrobot," *International Conference on Mechatronics and Automation*, pp. 509–514.
- [10] Kamamichi, N., Yamakita, M., Asaka, K., and Luo, Z. W., 2006, "A Snake-Like Swimming Robot Using IPMC Actuator/Sensor," *International Conference on Robotics and Automation (ICRA 2006)*, Orlando, FL, May 15–19, pp. 1812–1817.
- [11] Chang, Y. C., and Kim, W. J., 2013, "Aquatic Ionic-Polymer–Metal-Composite Insectile Robot With Multi-DOF Legs," *IEEE-ASME Trans. Mechatron.*, 18(2), pp. 547–555.
- [12] Guo, S., Shi, L., Xiao, N., and Asaka, K., 2012, "A Biomimetic Underwater Microrobot With Multifunctional Locomotion," *Robot. Auton. Syst.*, 60(12), pp. 1472–1483.
- [13] Okazaki, K., Ogiwara, T., Yang, D., Sakata, K., Saito, K., Sekine, Y., and Uchikoba, F., 2011, "Development of a Pulse Control-Type MEMS Microrobot With a Hardware Neural Network," *Artif. Life Rob.*, 16(2), pp. 229–233.
- [14] Kohut, N. J., Hoover, A. M., Ma, K. Y., Baek, S. S., and Fearing, R. S., 2011, "Medic: A Legged Millirobot Utilizing Novel Obstacle Traversal," *IEEE International Conference on Robotics and Automation (ICRA)*, Shanghai, May 9–13, pp. 802–808.
- [15] Hoover, A. M., Steltz, E., and Fearing, R. S., 2008, "RoACH: An Autonomous 2.4 g Crawling Hexapod Robot," *IEEE/RSJ International Conference on Intelligent Robots and Systems (IROS 2008)*, Nice, France, Sept. 22–26, pp. 26–33.

- [16] Baisch, A. T., Sreetharan, P. S., and Wood, R. J., 2010, "Biologically-Inspired Locomotion of a 2g Hexapod Robot," IEEE/RSJ International Conference on Intelligent Robots and Systems (IROS), Taipei, Taiwan, Oct. 18–22, pp. 5360–5365.
- [17] Baisch, A. T., Heimlich, C., Karpelson, M., and Wood, R. J., 2011, "HAMR³: An Autonomous 1.7 g Ambulatory Robot," IEEE/RSJ International Conference on Intelligent Robots and Systems (IROS), San Francisco, CA, Sept. 25–30, pp. 5073–5079.
- [18] Baisch, A. T., Ozcan, O., Goldberg, B., Ithier, D., and Wood, R. J., 2014, "High Speed Quadrupedal Locomotion for a Microrobot," *Int. J. Rob. Res.*, **33**(8), pp. 1063–1082.
- [19] Otis, M. J. D., 2013, "Electromechanical Characterization and Locomotion Control of IPMC BioMicroRobot," *Adv. Mater. Sci. Eng.*, **2013**, p. 683041.
- [20] Panwar, V., Cha, K., Park, J. O., and Park, S., 2012, "High Actuation Response of PVDF/PVP/PSSA Based Ionic Polymer Metal Composites Actuator," *Sens. Actuators B*, **161**(1), pp. 460–470.
- [21] Panwar, V., Kang, B. S., Park, J. O., and Park, S. H., 2011, "New Ionic Polymer–Metal Composite Actuators Based on PVDF/PSSA/PVP Polymer Blend Membrane," *Polym. Eng. Sci.*, **51**(9), pp. 1730–1741.
- [22] Panwar, V., Lee, C., Ko, S. Y., Park, J. O., and Park, S., 2012, "Dynamic Mechanical, Electrical, and Actuation Properties of Ionic Polymer Metal Composites Using PVDF/PVP/PSSA Blend Membranes," *Mater. Chem. Phys.*, **135**(2), pp. 928–937.
- [23] Panwar, V., Ko, S. Y., Park, J. O., and Park, S., 2013, "Enhanced and Fast Actuation of Fullerene/PVDF/PVP/PSSA Based Ionic Polymer Metal Composite Actuators," *Sens. Actuators B*, **183**, pp. 504–517.
- [24] Murthy, R., Das, A., and Popa, D. O., 2008, "ARRIpede: A Stick-Slip Micro Crawler/Conveyor Robot Constructed Via 2 1/2D MEMS Assembly," IEEE/RSJ International Conference on Intelligent Robots and Systems (IROS 2008), Nice, France, Sept. 22–26, pp. 34–40.
- [25] Moeinkhah, H., Jung, J. Y., Jeon, J. H., Akbarzadeh, A., Rezaeepazhand, J., Park, K. C., and Oh, I. K., 2013, "How Does Clamping Pressure Influence Actuation Performance of Soft Ionic Polymer–Metal Composites?" *Smart Mater. Struct.*, **22**(2), pp. 25014–25015.
- [26] Bennett, M., and Leo, D., 2005, "Morphological Characterization of Ionic Liquid and Electromechanical/Nafion Polymer Composites," *Proc. SPIE*, **5759**, pp. 506–517.